

## Oscillatory interaction of steps on W{110}

Wei Xu\* and James B. Adams

*Department of Materials Science and Engineering, University of Illinois at Urbana-Champaign, 105 South Goodwin Avenue, Urbana, Illinois 61801*

T. L. Einstein

*Department of Physics, University of Maryland, College Park, Maryland 20742-4111*

(Received 21 February 1996)

Using a modified fourth-moment approximation to tight-binding theory, we have carried out a systematic study of the energetics of steps and kinks on the W{110} surface. This model predicts an oscillatory interaction (as a function of separation) between isolated stable steps on the W{110} surface, whereas previous studies of step-step interactions on late transition and noble metals with the embedded atom method found a purely repulsive, inverse-square decay. The oscillations are similar to those found by scanning tunneling microscope measurements of vicinal Cu{100} and Ag{110} systems. [S0163-1829(96)05228-9]

### I. INTRODUCTION

The study of the energetics of steps, kinks, and step-step interactions on metal surfaces is very important because these energies provide the key to understanding equilibrium surface structures, surface roughening, and the dynamics of crystal growth. Recently, the availability of the scanning tunneling microscope (STM) has made it possible to measure such energies.<sup>1-7</sup> STM observations of semiconductor surfaces<sup>1-4</sup> indicated that step-step interactions were purely repulsive, decaying inversely with the square of their separation, indicative of entropic and elastic mechanisms. However, similar studies of some metallic systems revealed a more complicated interaction between steps.<sup>6,7</sup> Frohn and co-workers<sup>6</sup> measured the distribution of terrace widths on vicinal Cu{100} surfaces using a STM. They found that the distribution does not scale simply with the mean terrace width and so are not produced simply by inverse-square repulsions. Instead, the step-step interactions can be interpreted as repulsive at short distances and attractive at larger separations of 3-5 atomic spacings. In their study of vicinal Ag{110} surfaces, Pai *et al.*<sup>7</sup> similarly concluded that interactions did not decay monotonically and were attractive at intermediate spacings. Furthermore, they noted that in this case the oscillatory interactions could be described as indirect electronic interactions, the envelope of which decayed unusually slowly because a surface state near the Fermi energy (and in the correct direction) mediated the interaction.

Much theoretical work has been motivated by these intriguing STM measurements. Most of these studies concentrated on the fcc transition metals, both because the experiments were on these systems and because the semiempirical methods usually used are most suitable for these elements. For example, the embedded-atom method (EAM) has been used to calculate step formation energy and step-step interactions on Cu{100},<sup>8</sup> Ag{100}, and Ag{111} (Ref. 9) and other fcc metal surfaces.<sup>10-12</sup> Similarly, faceting on the Au{11n} surfaces has been studied using the similar glue model.<sup>13</sup> The step formation energy and step-step interactions on Cu{113} and {115} were calculated using an  $N$ -body

potential.<sup>14</sup> The energetics of steps and kinks on Ag and Pt were also investigated using equivalent crystal theory.<sup>15</sup> In these calculations, the interaction potentials between steps on the metal surfaces are dominated by a repulsive term, which, in general, can be described with a  $r^{-2}$  term. (Here  $r$  is the separation between two steps.) However, they failed to yield an attractive force between steps at intermediate separation, as found in STM measurements.<sup>6,7</sup>

In this paper we report an investigation of the energetics of steps and their interactions on a W{110} surface. Our calculations indicate that the interaction potential has oscillatory behavior, dominated by an  $r^{-2}$  term plus an oscillatory modulation, compatible with STM observations.

This paper is arranged as follows. The theoretical approach used in this work will be described in Sec. II. The results of step and kink formation energies on the W{110} surface will be reported in Sec. III. Section IV discusses the interaction between two steps. Finally, conclusions will be drawn in Sec. V.

### II. THEORETICAL MODEL

The model used in this work is based on the low-order moments approximation to tight-binding theory. Complete details of the fourth-moment method are contained in the paper by Xu and Adams.<sup>16</sup> The method builds on earlier work by Carlsson<sup>17</sup> and Foiles.<sup>18</sup> The total energy is given by

$$E = \frac{1}{2} \sum_{i,j} V_{\text{pair}}(r_{ij}) + E^{(2)} + E^{(3)} + E^{(4)}. \quad (1)$$

Here  $V_{\text{pair}}(r_{ij})$  is a pair interaction between pairs of ions separated by a displacement  $r_{ij}$ . The second-, third- and fourth-moment terms of the electronic density of states [ $E^{(2)}$ ,  $E^{(3)}$ , and  $E^{(4)}$  in Eq. (1)] are evaluated by taking double, triple, and quadruple products of tight-binding matrix elements of the  $d$  orbitals, which are formulated in Ref. 16. These moment terms represent the angular components of the interatomic interactions. In general, EAM-type poten-

tials include only the first two terms in Eq. (1), without the third- and fourth-moment terms in their Hamiltonians. The parameters in this fourth-moment method were determined empirically by fitting to many bulk properties. In previous papers,<sup>16,19,20</sup> this fourth-moment method has successfully yielded the  $W\{100\}(\sqrt{2}\times\sqrt{2})R45^\circ$  surface reconstruction, reasonable activation energies for single adatom self-diffusion on the  $W\{110\}$ ,  $\{211\}$ , and  $\{321\}$  surfaces, adatom-adatom interactions, and dimer diffusion on  $W\{110\}$  and  $\{211\}$  surfaces.

The computational method used in this work will be briefly introduced as follows. The  $W\{110\}$  surface is modeled by creating a slab with two free surfaces and periodic boundary conditions in the two directions parallel to the surface. The periodic length is held fixed at the bulk value. The  $N$ -atom slab is 25 Å thick (along the  $z$  direction) with about 1200 total atoms. The  $x$ - $y$  plane is about  $15\times 45$  Å<sup>2</sup>, with steps parallel to the  $x$  direction. Energy minimization by a conjugate gradient method is used to determine the stable structure of this system.

### III. ENERGETICS OF PRINCIPAL STEPS AND KINKS ON $W\{110\}$

The surface structure of  $W\{110\}$  has been reported in an earlier paper.<sup>20</sup> In general, the calculated multilayer relaxations are in reasonable agreement with experimental results. Three different step orientations on  $\{110\}$  surfaces have been considered in this study. Figure 1 shows the top view of these three steps with their orientations along the  $[111]$ , which is the closed packed direction,  $[110]$ , and  $[001]$ . To calculate the formation energy, we add a half-monolayer strip of atoms onto the fully relaxed  $\{110\}$  surface with the direction of the pair of up and down steps along  $[111]$ ,  $[001]$ , and  $[110]$ , respectively. Then, the whole system is relaxed freely to find the ground-state energy ( $E_{\text{step}}$ ). As discussed, e.g., in Ref. 9, the step formation energy  $G_{\text{step}}$  at 0 K (Ref. 21) can be constructed as

$$G_{\text{step}} = 2L\beta_{\text{step}} = (E_{\text{step}} - N_{\text{step}}E^{\text{coh}} - 2A\gamma_{(110)}). \quad (2)$$

Here  $L$  is the length of the step,  $\beta_{\text{step}}$  is the step formation energy per length,  $N_{\text{step}}$  is the number of atoms in this system, and  $E^{\text{coh}}$  is the bulk cohesive energy. For the orientations we consider, the up and the down steps are geometrically equivalent, enabling us simply to include the factor of 2 to account for the two of them. The factor  $2A\gamma_{(110)}$  is determined from a calculation of the energy of a slab bounded by flat  $\{110\}$  surfaces:

$$2A\gamma_{(110)} = E_{\text{surf}} - N_{\text{surf}}E^{\text{coh}}, \quad (3)$$

where  $A$  is the surface area of each side of the slab,  $\gamma_{(110)}$  is the  $\{110\}$  surface energy per area, and  $N_{\text{surf}}$  is the number of atoms of this flat  $\{110\}$  slab (without the extra half layer).

Table I lists the calculated step formation energies for three steps along the  $[111]$ ,  $[110]$ , and  $[001]$ , on a  $\{110\}$  surface, specifically a  $(\bar{1}10)$  plane, as illustrated in Fig. 1. The microfacet orientations for these steps are  $\{110\}$ ,  $\{112\}$ , and  $\{001\}$ , respectively. An obvious feature found in Table I is that the  $[111]$  step has the lowest formation energy (136 meV/Å) compared with the other two (208 and 309 meV/Å).

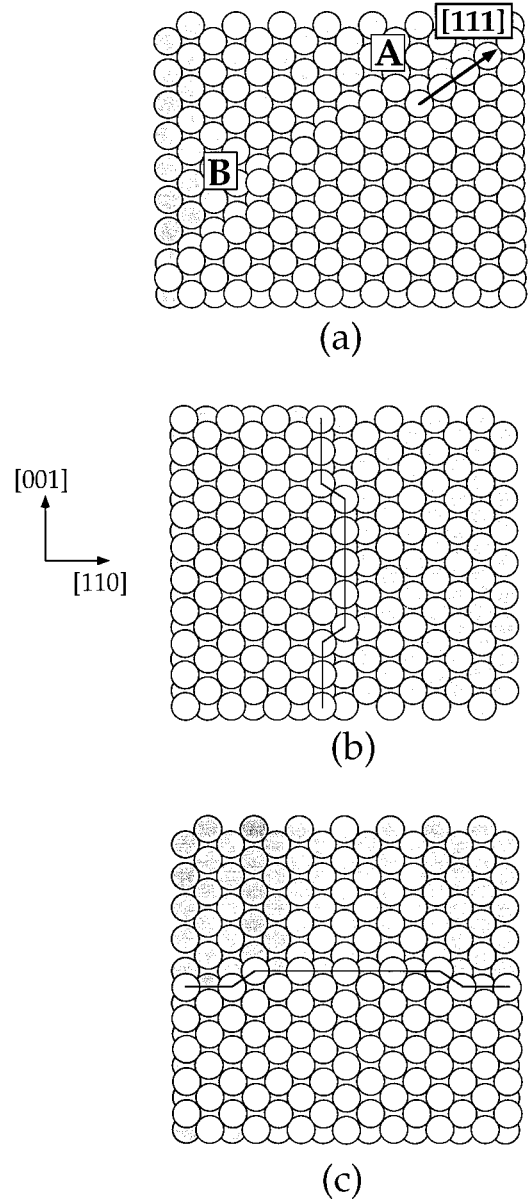


FIG. 1. Schematic of steps and kinks on the  $W\{110\}$  surface: (a)  $[111]$  step with kink (A) and antikink (B), (b)  $[001]$  step with kink, and (c)  $[110]$  step with kink.

Thus, as expected from Ref. 9, the step energy increases as the planar density of the microfacet decreases. While simple bond coordination models can sometimes be misleading, we note that on a bcc  $\{110\}$  surface, each ledge atom on the  $[111]$  step has 5 nearest neighbors (NN's). When  $[110]$  and  $[001]$  steps are formed on this surface, however, the number of NN's changes to 4 with one extra bond to be broken. These two steps thus will require much higher formation energy compared to that of a step along the close-packed  $[111]$  direction.

The step formation energy can be estimated using the ‘‘awning’’ approximation.<sup>9</sup> We briefly summarize this approach here; further details can be found in Ref. 9. One starts with the free energy per area of the microfacet of the step riser planes connecting atoms at the top and bottom ‘‘creases’’ of a step, multiplied by the distance  $d$  across the riser. From this one subtracts the free energy per area of the

TABLE I. Formation energies of a step and a kink on  $W\{110\}$  at 0 K.

Step formation energy (meV/Å)		Kink formation energy (meV)		
[111] step	136	on [111] step	kink	349
[110] step	208		antikink	427
[001] step	309	on [110] step		-288
		on [001] step		-275

terrace plane times the projection of  $d$  onto the terrace plane (i.e.,  $d$  times the cosine of the tilt of the microfacet). For a simple [110] step, the riser is a {112} microfacet with  $d = (\sqrt{3}/2)a$ , where  $a = 3.165 \text{ \AA}$  is the lattice constant for bulk W. We find, in this case, that the free energy per unit length of step formation can be approximated as

$$\beta_{[110]/(110)} \approx \left[ \frac{\sqrt{3}}{2} \gamma_{(112)} - \frac{1}{2} \gamma_{(110)} \right] a, \quad (4)$$

where  $\gamma_{(112)}$  and  $\gamma_{(110)}$  are the surface energies per unit area of the {112} and the {110} planes, which have the values 137 and 116 meV/Å<sup>2</sup>, respectively. The estimate of  $\beta$  for the [110] step is 192 meV/Å, close to the calculated value in Table I. Similarly, the step formation energy for [111] and [001] steps on the {110} surface are

$$\beta_{[111]/(110)} \approx \left[ \frac{\sqrt{6}}{3} \gamma_{(110)} - \frac{\sqrt{6}}{6} \gamma_{(110)} \right] a = 0.4082 \gamma_{(110)} a \quad (5)$$

and

$$\beta_{[001]/(110)} \approx \left[ \gamma_{(001)} - \frac{\sqrt{2}}{2} \gamma_{(110)} \right] a \quad (6)$$

and the surface energy of the {001} plane is 217 meV/Å<sup>2</sup>. The estimated  $\beta$ 's for these two steps are 150 and 427 meV/Å, respectively. The awning estimates, while fair, are not as good as for late transition and noble metals because the directionality of bonds is much more important for W.

In a two-dimensional zero-temperature Wulff plot, we would quickly find that the [111] step provides the dominant ‘‘facet,’’ i.e., edge. Moreover, closer inspection shows that if  $\beta_{[111]} < \sqrt{2/3} \beta_{[110]}$ , there will be no [110] edge on the equilibrium crystal shape, where the numerical factor comes from the inner product of the unit direction vectors of the two steps. This inequality is in fact satisfied by the numbers in Table I. Likewise, since  $\beta_{[111]} < \sqrt{1/3} \beta_{[001]}$ , there will be no [001] edge. Presumably, no other lower-symmetry orientation is stable either. In other words, the fourth-moment calculations predict that the only stable step orientation at 0 K is [111], so that the equilibrium two-dimensional crystal shape is a diamond. (At finite temperature, we expect these statements to remain excellent approximations, though, of course, the facet will be rounded by finite-temperature roughening.) We shall see next that the instability of the [110] and the [001] steps in these calculations is reflected by their negative kink energies. Experimentally, there are no direct measurements of isolated single steps on the  $W\{110\}$  surface. However, low-energy electron diffraction studies of the  $W\{430\}$  surface, which can be treated as [001] steps uniformly separated on {110} surface, revealed no roughness for

[001] steps.<sup>22</sup> Since the separation of [001] steps ( $\sim 16 \text{ \AA}$ ) on {430} surface is rather large, it seems unlikely that interactions between [001] steps reduce this discrepancy. This issue certainly demands further investigation.

To compute the kink formation energy  $G_{\text{kink}}$  at 0 K, we use two methods. When we remove a half row of atoms from one step, it will actually create two kinks in the simulation cell, due to the periodic boundary condition (Fig. 1). Two kinks created in the simulation cell on [110] or [001] steps are equivalent to each other, i.e., have the same microfacet structure. Therefore,  $G_{\text{kink}}$  can be calculated using this expression

$$G_{\text{kink}} = (E_{\text{kink}} - N_{\text{kink}} E^{\text{coh}} - 2A \gamma_{(110)} - 2L \beta_{\text{step}}) / 2, \quad (7)$$

where  $N_{\text{kink}}$  is the total number of atoms in this system and  $E_{\text{kink}}$  is the total energy of the system in the ground state. The  $A \gamma_{(110)}$  and  $L \beta_{\text{step}}$  are the formation energy of surface and step, which have been given in Eqs. (2) and (3). The distance between kinks is over 15 Å. The kink formation energies on the [110] and [001] steps are listed in Table I.

For [111] steps there are two kinds of kinks: kinks and antikinks. As shown in Fig. 1(a), a kink ( $A$ ) is a simple unit deviation of the step along the ‘‘other’’ [111] direction on the surface. To return to the original step requires a unit deviation along the higher-energy [100] direction; we call it an antikink ( $B$ ). Alternatively, the antikink can be viewed as returning to the original step one atom sooner, along the same [111] direction as the kink, along a ‘‘Z-shaped’’ path, forming an acute rather than obtuse angle with the step. This perspective turns out to produce a lower energy in the awning approximation that is closer to the computed value. Since a kink-antikink pair will be created using periodic boundary conditions (i.e., by adding or removing half a chain of atoms), we need to adopt a different method to obtain the isolated kink or antikink formation energy. We could use a slab with a high Miller index associated with an azimuthal twist, but it is easier to use a large cluster on the {110} plane with its four edges along different  $\langle 111 \rangle$  directions. The length of each edge is over 20 Å. Then, an isolated kink or antikink can be created in one edge. Similarly,  $G_{\text{kink}}$  can be written as

$$G_{\text{kink}} = E_{\text{kink}} - N_{\text{kink}} E^{\text{coh}} - 2A \gamma_{(110)} - L \beta_{\text{step}}, \quad (8)$$

where  $L$  is the total ledge length of the cluster and other terms have the same definition as Eq. (7). Table I gives the formation energies of single kink and antikink on a [111] step.

One feature observed from Table I is that the [110] and [001] steps possess negative kink formation energies, in contrast to that on [111] step. This negativity simply indicates the [110] and [001] steps are energetically unstable in this

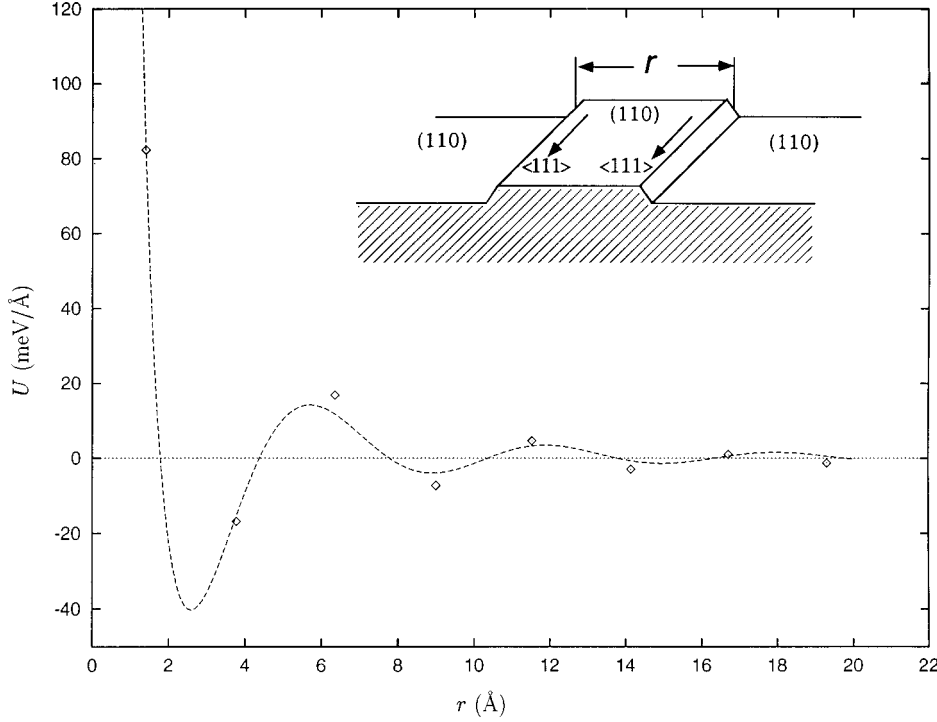


FIG. 2. “Mesa” step-step interaction potential  $U(r)$  shown (diamond points) as a function of step separation  $r$  on the W{110} surface. The dashed line is from Eq. (14), using parameters listed in Table III.

calculational method, decaying into segments with the stable orientation. In the other words, the [111] step, in which the step ledge is running in the [111] direction, will be very smooth and have a very low density of thermally excited kinks. In contrast, the [110] and [001] steps, as well as steps in any other direction, would form a large-scale zigzag pattern with a high densities of kinks. To understand the difference in kink formation energies, we first count the bond coordination change when a kink is created. Then an “awning”-type argument is used to give quantitative estimates. Qualitatively, when a kink is formed on the [111] step, one NN bond will be broken with the total NN’s for the outer corner kink atom changing from 5 to 4 and the other ledge atoms retain the same NN’s. The formation energy therefore is a positive value. In contrast, during the formation of a kink on the [110] and [001] steps, the number of NN’s will increase by one (5 NN’s for the inner corner kink atom vs 4 NN’s for a ledge atom). Thus it is energetically more favorable to form a kink on the [110] and [001] steps with formation energies of  $-288$  and  $-275$  meV per kink, respectively.

Similar to the estimates of step formation energy using an awning approximation, the kink formation energies on [111], [110], and [001] steps can be approximated as

$$G_{\text{kink}}^{[111]} \approx \left[ \frac{\sqrt{3}}{2} \beta_{[111]} - \frac{\sqrt{3}}{6} \beta_{[111]} \right] a = \frac{\sqrt{3}}{3} \beta_{[111]} a, \quad (9)$$

$$G_{\text{antikink}}^{[111]} \approx \left[ \frac{\sqrt{3}}{2} \beta_{[111]} + \frac{\sqrt{3}}{6} \beta_{[111]} \right] a = \frac{2\sqrt{3}}{3} \beta_{[111]} a$$

$$\approx \left[ \beta_{[100]} - \frac{\sqrt{3}}{3} \beta_{[111]} \right] a, \quad (10)$$

$$G_{\text{kink}}^{[110]} \approx \left[ \frac{\sqrt{3}}{2} \beta_{[111]} - \frac{\sqrt{2}}{2} \beta_{[110]} \right] a, \quad (11)$$

$$G_{\text{kink}}^{[001]} \approx \left[ \frac{\sqrt{3}}{2} \beta_{[111]} - \frac{1}{2} \beta_{[001]} \right] a. \quad (12)$$

Such simple estimates will give the kink formation energies to be 249 meV for a kink and 497 meV (or 730 meV if one chooses the [100] perspective) for an antikink on a [111] step  $-93$  and  $-116$  meV on [110] and [001] steps, respectively, which agree qualitatively with the full calculation based on Eqs. (7) and (8).

#### IV. INTERACTION BETWEEN [111] STEPS ON THE W{110} SURFACE

Using this fourth-moment method, we studied the interaction potential of two isolated straight [111] steps as a function of their separation. There are three possible geometries for two isolated steps. As shown in the inset of Fig. 2, the first type involves an up and down pair, with the region between them elevated above the surface by one layer; we call this the “mesa” configuration. The second type, illustrated in the inset of Fig. 3, has a down and up pair, with the intervening region depressed by a layer; we call this a “dado” configuration. Such interactions occur across islands and pits, respectively, on the surface. The third type of step-step interaction, having two ups (or two downs), is shown in the inset of Fig. 4. It would occur on a vicinal surface and is called a “staircase” configuration.

To calculate the interaction between a mesa pair, we first create two [111] steps on the {110} surface, separated by 20 Å. The distance between steps is defined as the distance between the midpoints of the riser planes. The ground-state energy of this fully relaxed system of  $N_{\infty}$  atoms is denoted as

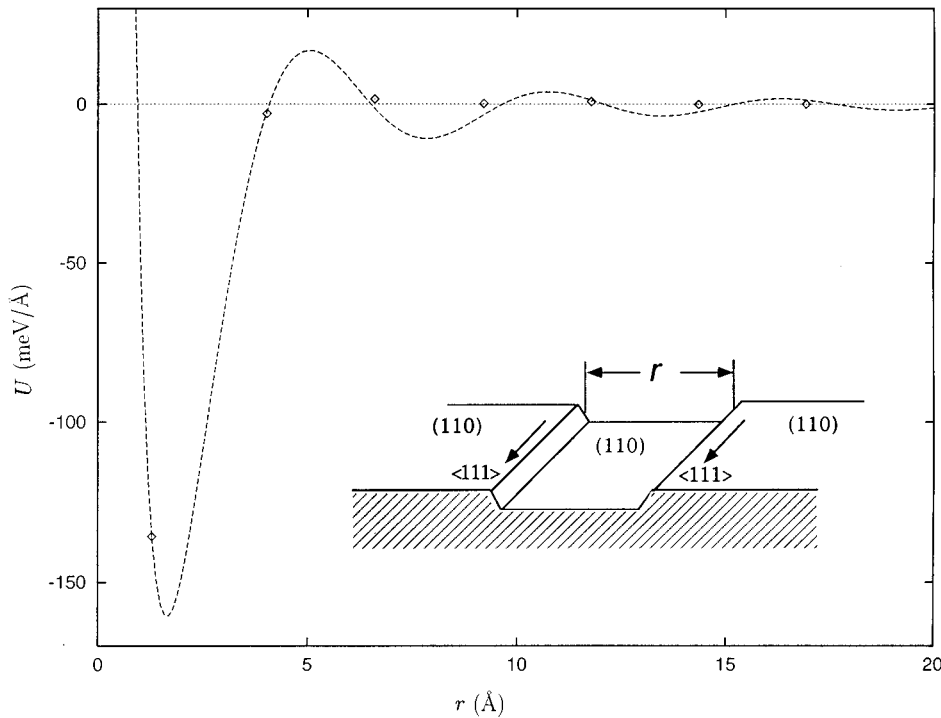


FIG. 3. "Dado" step-step interaction potential  $U(r)$  shown (diamond points) as a function of step separation  $r$  on the W{110} surface. The dashed line is from Eq. (14), using parameters listed in Table III.

$E_\infty$ . Then, we reduce the separation between the two steps by removing atomic rows and relaxing the new structure (total energy denoted as  $E_I$  with  $N_I$  atoms). The interaction can be written as:

$$U_I = \frac{1}{2L} [E_I - E_\infty - (N_I - N_\infty)E^{\text{coh}}]. \quad (13)$$

Figure 2 shows the interaction potential as a function of separation  $r$ . Basically, the interaction potential can be treated as a monotonic repulsive function plus a decaying

oscillatory modulation. At  $r = 1.4 \text{ \AA}$ , only one linear adatom row is left on the {110} surface and the interaction is a very strong repulsion (82.3 meV/Å); this indicates that such a linear pattern of adatoms on the {110} surface is very unfavorable energetically. With the separation increased to  $r = 3.77 \text{ \AA}$ , two steps will attract each other with an interaction energy of  $-16.8 \text{ meV/Å}$ . Thereafter, the interaction oscillates between repulsive and attractive out to very large separations.

Similarly, we can calculate the interactions for dado pairs as a function of separation  $r$ . In this case,  $E_\infty$  is the ground-

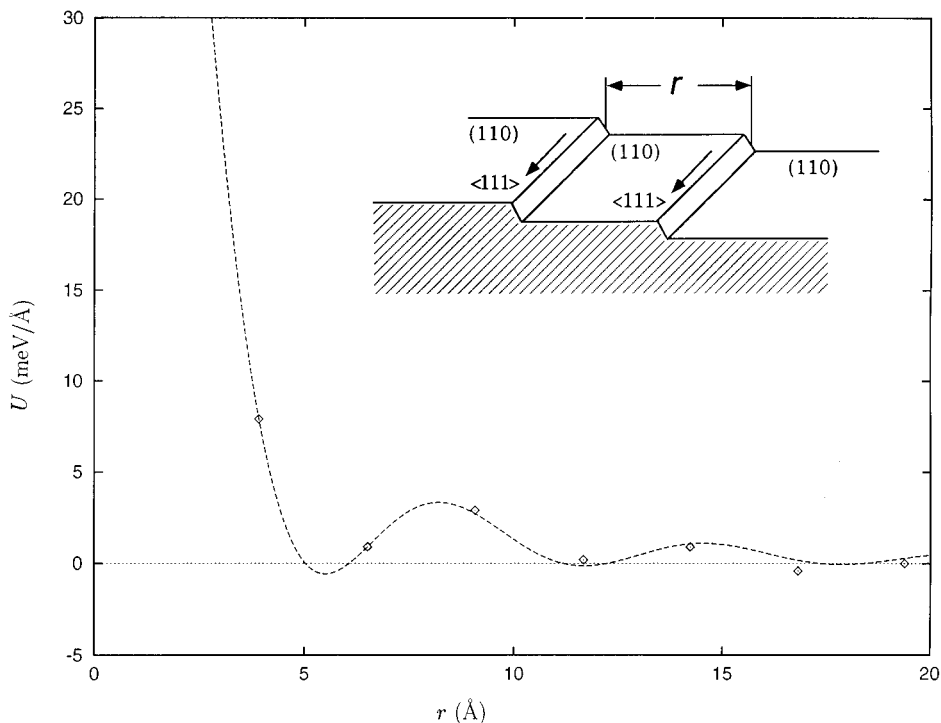


FIG. 4. "Staircase" step-step interaction potential  $U(r)$  shown (diamond points) as a function of step separation  $r$  on the W{110} surface. The dashed line is from Eq. (14), using parameters listed in Table III.

TABLE II. Step-step interactions in the three configurations as a function of their separation.

Rigid $r_0$ (Å)	Mesa		Dado		Staircase	
	$r$ (Å)	$U$ (meV/Å)	$r$ (Å)	$U$ (meV/Å)	$r$ (Å)	$U$ (meV/Å)
1.29	1.40	82.3	1.29	-135.8		
3.88	3.77	-16.8	4.03	-2.9	3.91	7.9
6.46	6.35	16.8	6.59	1.6	6.50	0.9
9.05	8.99	-7.3	9.20	0.2	9.06	2.9
11.63	11.52	4.6	11.77	0.8	11.67	0.2
14.21	14.13	-3.0	14.35	-0.1	14.23	0.9
16.80	16.69	1.0	16.93	0.0	16.81	-0.4
19.38	19.29	-1.3			19.38	0.0

state energy with the two steps separated by 20 Å. The interaction potential also shows oscillatory behavior for dado steps. The minimum distance between two dado steps is 1.29 Å, which actually is the nearest distance between two [111] atom rows on a {110} plane. The interaction at  $r=1.29$  Å is -135.8 meV/Å. When  $r$  increases to 4.03 Å, the interaction is still attractive with a magnitude of -2.9 meV/Å. At large  $r$ , the interaction changes to repulsive and then fluctuates as seen in Fig. 3.

Unlike the previous two types of steps, most of the interactions between staircase pairs are repulsive, with a small attraction at  $r=16.81$  Å. (See Table II.) Figure 4 shows the interaction potential as a function of separation  $r$ . (Here  $r$  is just the lateral separation and does not include the vertical component.) The staircase interactions also exhibit the main feature observed in mesa and dado interactions: oscillatory behavior. At the nearest separation (3.91 Å), the interaction between two steps is a repulsion of 7.9 meV/Å. When  $r$  increases to 6.5 Å, the repulsion reduces to 0.9 meV/Å. The interaction oscillates back to 2.9 meV/Å at  $r=9.06$  Å and then decreases again as seen in Fig. 4.

Two experimental studies found that the interaction potential between two steps on particular noble metal surfaces exhibits oscillatory behavior.<sup>6,7</sup> Evidently the step-step interactions are repulsive for small step separations and attractive at intermediate separations, in contrast to the step-step interactions on semiconductor surfaces, which show a monotonic  $r^{-2}$  repulsion due to elastic (or at least entropic) effects.<sup>1-4</sup> It has been suggested that the attractive step-step interactions can result from dipole-dipole interactions<sup>23,24</sup> or indirect electronic interactions.<sup>6,7,25,26</sup>

Figures 2–4 show that the interactions between two isolated steps on the W{110} surface do not simply decay monotonically with increasing separation. Instead, they can be modeled as a monotonic function plus an oscillatory modulation. In order to establish the source and form of the interactions, we fit a general form to the “data” produced by the fourth-moment method. Following the arguments by Pai *et al.*<sup>7</sup> and Einstein,<sup>26</sup> we choose the general form as

$$U(r) = \frac{A}{r^2} + \frac{B \cos(2kr + \delta)}{r^m}. \quad (14)$$

Here  $A$ ,  $B$ ,  $m$ ,  $k$ , and  $\delta$  serve as fitting parameters. The  $r^{-2}$  term is the elastic or dipolar interaction. The second term in Eq. (14) has the Ruderman-Kittel-Kasuya-Yosida-like form<sup>27</sup> characteristic of indirect interactions in the as-

ymptotic limit;  $k$  is the Fermi wave vector with velocity in the direction of the interstep separation;  $\delta$  is associated with the localized perturbation. In fitting Eq. (14) to the results of the fourth-moment calculation, we found values of  $m$  rather close to 2 (and decidedly less than 5) for the three interaction potentials. While the indirect interaction is typically characterized by an envelope decaying as  $r^{-5}$ , it decays as  $r^{-2}$  when the interaction is mediated by surface states. (See footnote 27 in Ref. 7.) While, to our knowledge, there has been no computation of the surface electronic structure of W{110}, there have been such computations for its neighbor, Ta{110}.<sup>28,29</sup> There are some surface states in these calculations a couple eV about the Fermi level. They might be closer to it for W. Unfortunately, the computations were not performed in the direction associated with propagation between [111] steps, so it is not clear whether these states actually contribute to the step interaction. In any case, to simplify our argument, we set  $m$  to be 2. The fitting parameters for three interactions are listed in Table III. The dashed lines on Figs. 2–4 are from Eq. (14) using parameters listed in Table III. The agreement with the fourth-moment calculations is quite reasonable, consistent with the idea that the oscillations arise from indirect electronic interactions, as conjectured from experimental measurements.<sup>6,7</sup> Further positive evidence in Table III is the fact that the  $k$  values for three cases are similar, while the values for  $\delta$  differ considerably.

From Table II it is clear that relaxations of the individual steps play a notable role in these problems. For an isolated step, the top edge retracts both inward and downward (by about 0.01 Å), as one might expect from because of its decreased coordination. The atom at the base of the step moves about the same distance and direction horizontally, while rising twice as much. The lateral part of this shift can be seen in the decrease (except at the smallest separation) of separations

TABLE III. Parameters used in Eq. 14 for three types of step-step interactions.

Parameter	Mesa	Dado	Staircase
$A$ (meV Å)	84.51	-117.12	109.05
$B$ (meV Å)	406.44	568.99	126.43
$k$ (Å <sup>-1</sup> )	0.52	0.56	0.51
$\delta$	-0.03 $\pi$	0.10 $\pi$	-0.80 $\pi$
$m$	2	2	2

relative to the rigid lattice for the mesa configuration and the concomitant increase for the dado configuration. In the staircase configuration, both steps relax in the same direction, so there is less effect on their separation.

The elastic interaction, which can be described by the  $r^{-2}$  term in Eq. (14), only contributes partly to the step-step interactions on a metal surface. Indirect electronic interactions will dominate at longer separations. A simple EAM-type potential always yielded a monotonic interaction between steps for all the region and failed to predict such oscillatory behavior.<sup>8,9,12</sup> This is because the Hamiltonian in the EAM includes only a mean electronic density (like the second-moment term) contributed from its local environment. Although the fourth-moment model, which includes the higher moments (third and fourth) of the local electron density of states, is unable to provide detailed information about Fermi-surface singularities, it certainly is a considerable improvement over the EAM-type potentials in describing interaction energetics on transition-metal surfaces.

## V. CONCLUSION

We have studied the formation energies of steps and kinks and the interactions of steps on W{110} surface, using a recently developed theoretical model: the fourth-moment method. Our calculations indicate that a step with its orientation along the closed-packed [111] direction has a much

lower formation energy compared to other steps along [110] and [001]. On the other hand, it is much easier to form a kink on the [110] and [001] steps, with negative kink formation energies, than that on the [111] step. A simple theory based on the bond coordination change and an ‘‘awning’’ approximation can be used to understand the difference of those formation energies.

The present calculation shows that the interaction potentials between two isolated steps include two parts: (i) an elastic  $r^{-2}$  term and (ii) an oscillatory modulation  $r^{-m}\cos(2kr+\delta)$ . This is consistent with recent STM measurements, which found the step-step interactions on metal surfaces are repulsive for small step separations and attractive at intermediate step separations, unlike the step interactions on semiconductor surfaces. Our analysis supports the belief that the oscillations are due to indirect electronic interactions.

## ACKNOWLEDGMENTS

We would like to thank the National Center for Supercomputing Application for their help. This work was supported by the U.S. Department of Energy, Office of Basic Energy Sciences through the Materials Research Laboratory at the University of Illinois under Grant No. DE-A(O)-76ER01198. T.L.E. was supported by NSF MRG Grant No. DMR 91-03031.

\*Present address: Lawrence Livermore National Laboratory, University of California, Livermore, CA 94551.

<sup>1</sup>B. S. Swartzentruber, Y.-W. Mo, R. Kariotis, M. G. Lagally, and M. B. Webb, Phys. Rev. Lett. **65**, 1913 (1990).

<sup>2</sup>X. S. Wang, J. L. Goldberg, N. C. Bartelt, T. L. Einstein, and E. D. Williams, Phys. Rev. Lett. **65**, 2430 (1990).

<sup>3</sup>B. S. Swartzentruber, N. Kitamura, M. G. Lagally, and M. B. Webb, Phys. Rev. B **47**, 13 432 (1993).

<sup>4</sup>Y. N. Yang, B. M. Trafas, R. L. Siefert, and J. H. Weaver, Phys. Rev. B **44**, 3218 (1991).

<sup>5</sup>M. Poensgen, J. F. Wolf, J. Frohn, M. Giesen, and H. Ibach, Surf. Sci. **274**, 430 (1992).

<sup>6</sup>J. Frohn, M. Giesen, M. Poensgen, J. F. Wolf, and H. Ibach, Phys. Rev. Lett. **67**, 3543 (1991).

<sup>7</sup>W. W. Pai, J. S. Ozcomert, N. C. Bartelt, T. L. Einstein, and J. E. Reutt-Robey, Surf. Sci. **307-309**, 747 (1994).

<sup>8</sup>Z.-J. Tian and T. S. Rahman, Phys. Rev. B **47**, 9751 (1993).

<sup>9</sup>R. C. Nelson, T. L. Einstein, S. V. Khare, and P. J. Rous, Surf. Sci. **295**, 462 (1993).

<sup>10</sup>C.-L. Liu and J. B. Adams, Surf. Sci. **294**, 211 (1993).

<sup>11</sup>R. Najafabadi and D. J. Srolovitz, Surf. Sci. **317**, 221 (1994).

<sup>12</sup>D. Wolf and J. A. Jaszczak, Surf. Sci. **277**, 301 (1992).

<sup>13</sup>A. Bartolini, F. Ercolessi, and E. Tosatti, Phys. Rev. Lett. **63**, 872 (1989).

<sup>14</sup>B. Loisel, D. Gorse, V. Pontikis, and J. Lapujoulade, Surf. Sci. **221**, 365 (1989).

<sup>15</sup>S. V. Khare and T. L. Einstein, Surf. Sci. **314**, L857 (1994).

<sup>16</sup>W. Xu and J. B. Adams, Surf. Sci. **301**, 371 (1994); **311**, 441 (1994).

<sup>17</sup>A. E. Carlsson, in *Solid State Physics: Advances in Research and Applications*, edited by H. Ehrenreich and D. Turnbull (Academic, New York, 1990), Vol. 43; Phys. Rev. B **44**, 6590 (1991).

<sup>18</sup>S. M. Foiles, Phys. Rev. B **48**, 4287 (1993).

<sup>19</sup>N. A. W. Holzwarth, J. A. Chervenak, C. J. Kimmer, Y. Zeng, W. Xu, and J. B. Adams, Phys. Rev. B **48**, 12 136 (1993).

<sup>20</sup>W. Xu and J. B. Adams, Surf. Sci. **319**, 45 (1994); **319**, 58 (1994); **339**, 241 (1995); **339**, 247 (1995).

<sup>21</sup>The leading correction due to configurational entropy is noted, e.g., in Ref. 9. For a discussion of vibrational effects, see A. Kara, S. Durukanoglu, and T.S. Rahman (unpublished).

<sup>22</sup>E. Conrad (private communication).

<sup>23</sup>C. Jayaprakash, C. Rottman, and W. F. Saam, Phys. Rev. B **30**, 6549 (1984).

<sup>24</sup>D. E. Wolf and J. Villain, Phys. Rev. B **41**, 2434 (1990).

<sup>25</sup>A. C. Redfield and A. Zangwill, Phys. Rev. B **46**, 4289 (1992).

<sup>26</sup>T. L. Einstein, in *Physical Structure of Solid Surfaces*, edited by W. N. Unertl (Elsevier, Amsterdam, in press).

<sup>27</sup>M. A. Ruderman and C. Kittel, Phys. Rev. **96**, 99 (1954); K. Yosida, *ibid.* **106**, 893 (1957); J. H. Van Vleck, Rev. Mod. Phys. **34**, 681 (1962).

<sup>28</sup>J. B. A. N. van Hoof, S. Crampin, and J. E. Inglesfield, J. Phys. Condens. Matter **4**, 8477 (1992).

<sup>29</sup>C. J. Wu, L. H. Yang, J. E. Klepeis, and C. Mailhot, Phys. Rev. B **52**, 11 784 (1995).